cascaded with the plant to effectively move the $1/T_{\theta_2}$ zero to $s = -3$. The MATLAB commands are

```
acl= aa - ba*0.1*ca(3,:);          % Close alpha loop, K_α=.1
qfb= ss(acl,ba,ca(2,:),0);         % SISO system for q f.b.
z=3; p=1;
lag= ss(-p,1,z-p,1);               % Lag compensator
csys= series(lag,qfb);             % Cascade Comp. before plant
[a,b,c,d]= ssdata(csys);
k= logspace(-2,0,2000);
r= rlocus(a,b,c,d,k);
plot(r)
grid on
axis([-20,1,-10,10])
```

The root-locus plot is the same shape as Figure 4.4-3, and when the pitch-rate feedback gain is $k_q = 0.2$, the closed-loop transfer function is

$$\frac{q}{u} = \frac{203.2s(s + 10.0)(s + 1.027)(s + 0.0217)(s + 3)}{(s + 18.02)(s + 10.3)(s + 1.025)(s + 1.98 \pm j2.01)(s + 0.0107 \pm j0.0093)} \quad (1)$$

When the pole and zero close to $s = -1$ are canceled out, this transfer function is essentially the same as in Example 4.4-1 except that there is a zero at $s = -3$ instead of $s = -1$. This zero can be replaced by a zero at $s = -1$ once again, by placing the lag compensator in the feedback path. However, a zero at $s = -1$ produces a much bigger overshoot in the step response than the zero at $s = -3$. Therefore the flying qualities requirements on $T_{\theta_2}$ should be checked (see Section The Handling Qualities Requirements) to obtain some guidance on the position of the zero.

This example shows that the same short-period mode, as in Example 4.4-1, can be achieved with much less alpha feedback and less pitch-rate feedback. Also, the transfer function (1) shows that no additional modes are introduced. A dynamic compensator is the price paid for this. Section 4.3 shows that the $1/T_{\theta_2}$ zero will move with flight conditions, and so the compensator parameters may have to be changed with flight conditions. ■

### Lateral-Directional Stability Augmentation/Yaw Damper

Figure 4.4-4 shows the most basic augmentation system for the lateral-directional dynamics. Body-axis roll rate is fed back to the ailerons to modify the roll subsidence mode, and yaw rate is fed back to the rudder to modify the dutch roll mode (yaw damper feedback). The lateral (rolling) motion is not, in general, decoupled from the yawing and sideslipping (directional) motions. Therefore, the augmentation systems will be analyzed with the aid of the multivariable state equations (two inputs, ailerons and rudder, and two or more outputs), as implied by the figure. This analysis will be restricted to the simple feedback scheme shown in the figure; in a later section additional feedback couplings will be introduced between the roll and yaw channels.

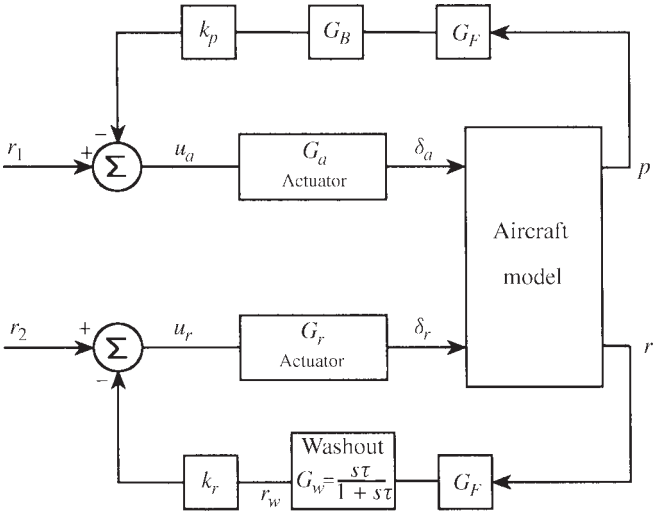


**Figure 4.4-4** Lateral-directional augmentation.

The purpose of the yaw damper feedback is to use the rudder to generate a yawing moment that opposes any yaw rate that builds up from the dutch roll mode. This raises a difficulty; in a coordinated steady-state turn the yaw rate has a constant nonzero value (see Table 3.6-3 and the subsection on turn coordination) which the yaw-rate feedback will try to oppose. Therefore, with the yaw damper operating, the pilot must apply larger than normal rudder pedal inputs to overcome the action of the yaw damper and coordinate a turn. This has been found to be very objectionable to pilots. A simple control system solution to the problem is to use "transient rate feedback," in which the feedback signal is differentiated (approximately) so that it vanishes during steady-state conditions. The approximate differentiation can be accomplished with a simple first-order high-pass filter (see Table 3.3-1), called a "washout filter" in this kind of application.

In Figure 4.4-4, $G_W$ is the washout filter, the transfer function $G_a$ represents an equivalent transfer function for differential actuation of the left and right ailerons, and $G_r$ is the rudder actuator. The transfer functions $G_F$ represent noise filtering and any effective lag at the output of the roll-rate and yaw-rate gyros, and $G_B$ is a *bending-mode filter*. The bending-mode filter is needed because the moments generated by the ailerons are transmitted through the flexible-beam structure of the wing, and their effect is sensed by the roll-rate gyro in the fuselage. The transfer function of this path corresponds to a general low-pass filtering effect, with resonances occurring at the bending modes of the wing. Because the wing bending modes are relatively low in frequency, they can contribute significant phase shift, and possibly gain changes, within the bandwidth of the roll-rate loop. The bending-mode filter is designed to compensate for these phase and gain changes.

To understand the purpose of the roll-rate feedback, consider the following facts. In Section 4.2 the variation of the roll time constant with flight conditions was

analyzed, and in Chapter 2 the change of aileron effectiveness with angle of attack was described. These effects cause large, undesirable variations in aircraft roll performance that result in the pilot flying the aircraft less precisely. Closed-loop control of roll rate is used to reduce the variation of roll performance with flight conditions.

While the roll time constant is a feature of the linear small-perturbation model and gives no indication of the maximum roll rate or time to roll through a large angle, it is relevant to the initial speed of response and control of smaller-amplitude motion. Figure 4.4-5 shows a plot of the reciprocal of the F-16 roll time constant versus alpha and indicates that this time constant may become unacceptably slow at high angles of attack. The plot was derived by trimming the F-16 model in straight and level flight at sea level, with the nominal cg position, over a range of speeds. At angles of attack greater than about 20° the roll pole coupled with the spiral pole to form a complex pair.

Landing approach takes place at a relatively high angle of attack, and the roll-rate feedback may be needed to ensure good roll response. Also, satisfactory damping of the dutch roll mode is particularly important during landing approach in gusty crosswind conditions. Our F-16 model does not include flaps and landing gear, so the design of the augmentation loops will simply be illustrated on a low-speed, low-altitude flight condition. If we take the F-16 model dynamics at zero altitude,

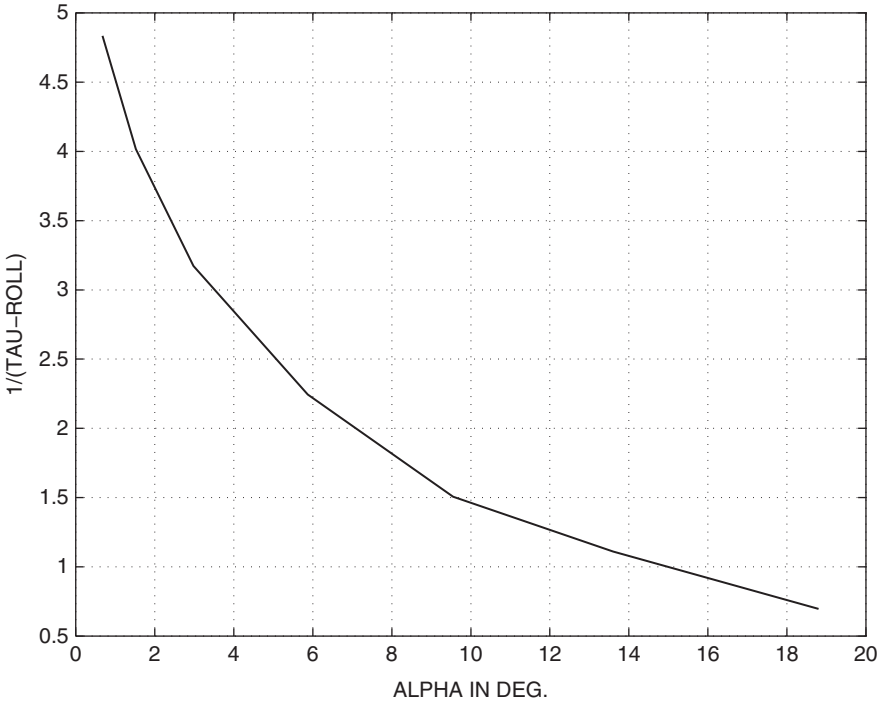


**Figure 4.4-5** F-16 model roll time constant versus alpha in degrees.

with the nominal cg position and an airspeed of 205.0 ft/s (alpha = 18.8°), the roll pole is real and quite slow ($\tau = 1.44$ s), and the dutch roll is very lightly damped ($\zeta = 0.2$). The state equations can be found by linearization, and a five-state set of lateral-directional equations can be decoupled from the full thirteen-state set. The coefficient matrices are found to be

$$A = \begin{array}{c} \begin{matrix} \beta & \phi & \psi & p & r \end{matrix} \\ \begin{bmatrix} -0.13150 & 0.14858 & 0.0 & 0.32434 & -0.93964 \\ 0.0 & 0.0 & 0.0 & 1.0 & 0.33976 \\ 0.0 & 0.0 & 0.0 & 0.0 & 1.0561 \\ -10.614 & 0.0 & 0.0 & -1.1793 & 1.0023 \\ 0.99655 & 0.0 & 0.0 & -0.0018174 & -0.25855 \end{bmatrix} \end{array}$$

$$B = \begin{array}{c} \begin{matrix} \delta_a & \delta_r \end{matrix} \\ \begin{bmatrix} 0.00012049 & 0.00032897 \\ 0.0 & 0.0 \\ 0.0 & 0.0 \\ -0.1031578 & 0.020987 \\ -0.0021330 & -0.010715 \end{bmatrix} \end{array} \tag{4.4-1a}$$

$$C = \begin{bmatrix} 0.0 & 0.0 & 0.0 & 57.29578 & 0.0 \\ 0.0 & 0.0 & 0.0 & 0.0 & 57.29578 \end{bmatrix} \begin{matrix} p \\ r \end{matrix} \qquad D = \begin{bmatrix} 0 & 0 \\ 0 & 0 \end{bmatrix} \tag{4.4-1b}$$

The null column in the $A$-matrix shows that the state $\psi$ is not coupled back to any other states, and it can be omitted from the state equations when designing an augmentation system. The $C$-matrix has been used to convert the output quantities to degrees, to match the control surface inputs. The transfer functions of primary interest are

$$\frac{p}{\delta_a} = \frac{-5.911(s - 0.05092)(s + 0.2370 \pm j1.072)}{(s + 0.06789)(s + 0.6960)(s + 0.4027 \pm j2.012)} \tag{4.4-2}$$

$$\frac{r}{\delta_a} = \frac{-0.1222(s + 0.4642)(s + 0.3512 \pm j4.325)}{(s + 0.06789)(s + 0.6960)(s + 0.4027 \pm j2.012)} \tag{4.4-3}$$

$$\frac{p}{\delta_r} = \frac{+1.202(s - 0.05280)(s - 2.177)(s + 1.942)}{(s + 0.06789)(s + 0.6960)(s + 0.4027 \pm j2.012)} \tag{4.4-4}$$

$$\frac{r}{\delta_r} = \frac{-0.6139(s + 0.5078)(s + 0.3880 \pm j1.5439)}{(s + 0.06789)(s + 0.6960)(s + 0.4027 \pm j2.012)} \tag{4.4-5}$$

The dutch roll poles are not canceled out of the $p/\delta_a$ transfer function by the complex zeros. Therefore, coupling exists between the rolling and yawing motions, and the dutch roll mode will involve some rolling motion. These transfer functions validate the decision to use the MIMO state equations for the analysis. At lower angles of

attack the dutch roll poles will typically be largely canceled out of the $p/\delta_a$ transfer function, leaving only the roll subsidence and spiral poles.

The two roll-rate transfer functions given above contain NMP zeros close to the origin. This is because gravity will cause the aircraft to begin to sideslip as it rolls. Then, if the dihedral derivative $C_{l_\beta}$ is negative (positive roll stiffness), the aircraft will have a tendency to roll in the opposite direction. This effect will be more pronounced in a slow roll when the sideslip has a chance to build up.

The rudder-to-roll-rate transfer function has another NMP zero farther away from the origin, corresponding to faster-acting NMP effects. A positive deflection of the rudder directly produces a positive rolling moment (see Table 3.5-1) and a negative yawing moment. The negative yawing moment rapidly leads to positive sideslip, which will in turn produce a negative rolling moment if the aircraft has positive roll stiffness. This effect tends to cancel the initial positive roll, and the NMP zero is the transfer function manifestation of these competing effects.

***Example 4.4-3: A Roll Damper/Yaw Damper Design*** In Figure 4.4-4 the aileron and rudder actuators will be taken as simple lags with a corner frequency of 20.2 rad/s (as in the original model), and the bending mode filter will be omitted. The coefficient matrices for the plant will be (4.4-1) with the $\psi$ state removed and denoted by *ap*, *bp*, *cp*, *dp*. Positive deflections of the control surfaces lead to negative values for the principal moments (Table 3.5-1) so, in order to use the positive-gain root locus for design, we will insert a phase reversal at the output of the control surface actuators (in the *C*-matrix). The aileron and rudder actuators will be combined into one two-input, two-output state model and cascaded with the plant as follows:

```
aa= [-20.2 0; 0 -20.2];    ba= [20.2 0; 0 20.2];        % Actuator
ca= [-1 0; 0 -1];          da= [0 0; 0 0];           % SIGN CHANGE
actua= ss(aa,ba,ca,da);                          % u1= δa, u2= δr
plant= ss(ap,bp,cp,dp);            % x1=beta, x2=phi, x3=p, x4=r
sys1 = series(actua,plant);                % y1=p, y2=r (degrees)
```

The washout filter will be incorporated in a two-input, two-output model, with the first input-output pair being a direct connection:

```
aw= [-1/τw];           bw= [0 1/τw];       % τw to be defined
cw= [0;-1];            dw= [1 0; 0 1];     % y1=p y2=washed-r
wash= ss(aw,bw,cw,dw);
sys2= series(sys1,wash);     % x1=wash, x2=beta,.., x6=ail, x7=rdr
```

The washout filter time constant is a compromise; too large a value is undesirable since the yaw damper will then interfere with the entry into turns. The following root-locus design plots can also be used to show that too small a value will reduce the achievable dutch roll damping (see Problem 4.4-3). The time constant is normally of the order of 1 s, and $\tau_W = 1.0$ s is used here.

Experience shows that the roll damping loop is the less critical loop, and it is conveniently closed first. The $p/u_a$ transfer function is the same as (4.4-2) with an

additional pole at $s = -20.2$ and the static loop sensitivity changed to 119 (i.e., 20.2 times the original value of 5.91). The MATLAB commands to obtain a root-locus plot and to close the loop are:

```
[a,b,c,d]= ssdata(sys2);
k= linspace(0,.9,3000);
r= rlocus(a,b(:,1),c(1,:),0,k);
plot(r)                          % Roll channel root locus
grid on
axis([-12,1,-5,5])
```

Figure 4.4-6 is the root-locus plot for positive $k_p$. It shows that the feedback has had the desired effect of speeding up the roll subsidence pole, which moves to the left in the $s$-plane and eventually combines with the actuator pole to form a complex pair. The spiral pole (not visible) moves a little to the right toward the NMP zero at $s = 0.05$, and the dutch roll poles change significantly as they move toward the open-loop complex zeros. If the feedback gain is made too high in this design, it will be found to be excessive at lower angles of attack. Furthermore, a high value will simply cause the aileron actuators to reach their rate and deflection limits more rapidly, as they become less effective at the higher angles of attack. A feedback gain

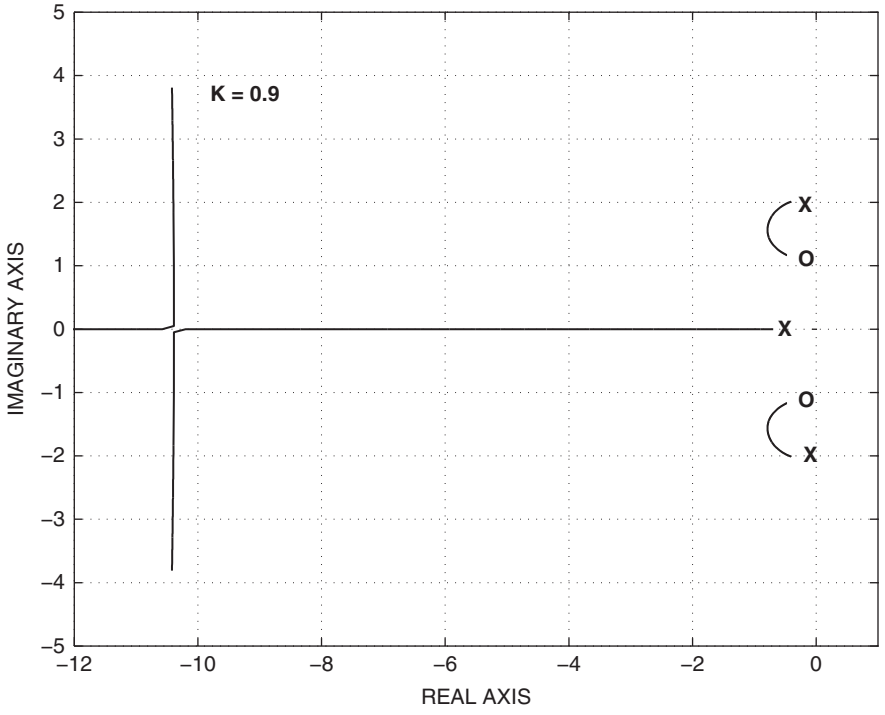


**Figure 4.4-6** Root-locus plot for the roll damping loop.

of $k_p = 0.2$ puts the roll subsidence pole at $s = -1.37$, which is about twice as fast as the open-loop value. This is a suitable starting value for investigating the effect of closing the yaw damper loop:

```
acl1= a - b(:,1)*k_p*c(1,:);              % Close roll loop
[z,p,k1]= ss2zp(acl1,b(:,2),c(2,:),0)   % Yaw tr. fn. + wash
r= rlocus( acl1,b(:,2),c(2,:),0,k);
plot(r)                                   % Yaw channel root locus
```

The transfer function $r_W/u_r$ (with $k_p = 0.2$) is

$$\frac{r_w}{u_r} = \frac{12.40s(s + 18.8)(s + 0.760)(s + 0.961 \pm j0.947)}{(s + 1)(s + 18.9)(s + 1.37)(s + 0.0280)(s + 20.2)(s + 0.752 \pm j1.719)} \quad (1)$$

A root-locus plot for closing the yaw-rate loop through the feedback gain $k_r$ is shown in Figure 4.4-7. Although not shown in the figure, one of the actuator poles is effectively canceled by the zero at $s = -18.8$; the remaining actuator pole moves to the right to meet the roll pole and form a new complex pair. As the magnitude of $k_r$ is increased, the spiral pole moves slightly closer to the washout zero at the origin, and the washout pole moves toward the zero at $s = -0.76$. At first the dutch roll poles

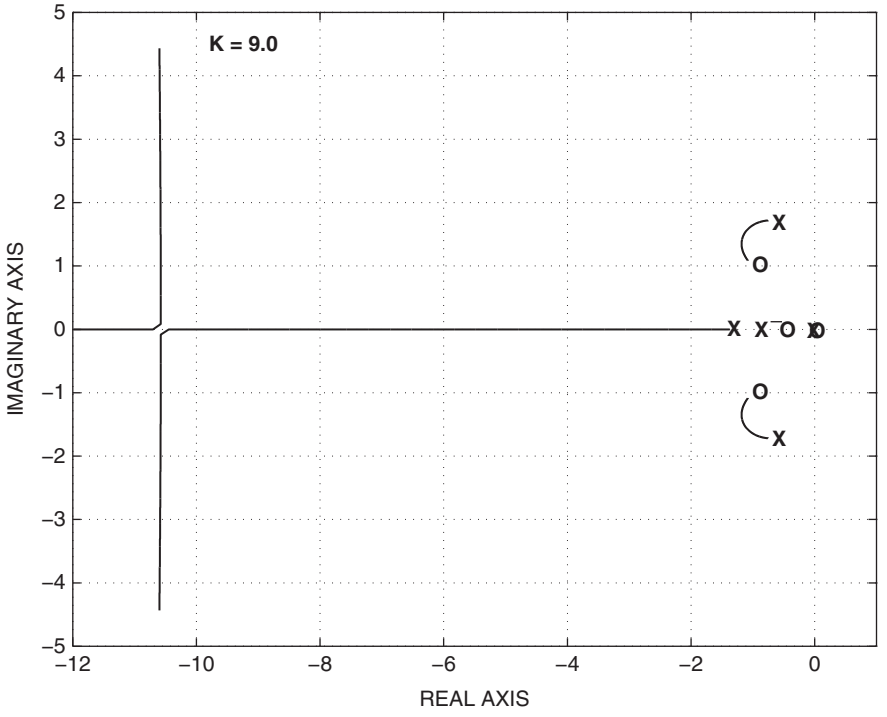


**Figure 4.4-7** Root-locus plot for the yaw-rate loop.

move around an arc of constant natural frequency (approximately), and increasing damping ratio, toward the complex zeros. After $k_r$ reaches about 3.5, the natural frequency begins to decrease and the damping ratio tends to remain constant. This feedback gain was considered to be the optimum value for the dutch roll poles, and so the yaw-rate loop was closed:

```
acl2= a - b*[.2 0; 0 3.5]*c;
[z,p,k1]= ss2zp(acl2,b(;,1),c(1,:),0)      % c.l. roll-rate t.f.
```

The principal transfer functions were found to be

$$\frac{p}{r_1} = \frac{119.4(\mathrm{s}+17.4)(\mathrm{s}-0.0502)(\mathrm{s}+3.74)(\mathrm{s}+0.262\pm \mathrm{j}0.557)}{(\mathrm{s}+18.7)(\mathrm{s}+17.7)(\mathrm{s}+0.0174)(\mathrm{s}+3.29)(\mathrm{s}+0.861)(\mathrm{s}+1.18\pm \mathrm{j}1.33)} \quad (2)$$

$$\frac{r}{r_2} = \frac{12.4(s+18.8)(s+1.00)(s+0.760)(s+0.961\pm j0.947)}{(s+17.7)(s+18.7)(s+3.29)(s+0.861)(s+0.0174)(s+1.18\pm j1.33)}, \quad (3)$$

where $r_1$ and $r_2$ are the roll-rate and yaw-rate reference inputs, as shown in Figure 4.4-4.

Transfer functions (2) and (3) show that the dutch roll poles and the washout pole (at $s = -0.861$) do not cancel out of the $p/r_1$ transfer function, so there is still strong coupling between the roll and yaw channels. The dutch roll natural frequency and damping ($\omega_n = 1.78$ rad/s, $\zeta = 0.67$) are now satisfactory, but the appearance of the relatively slow washout pole in the lateral dynamics may mean that the roll response is not much improved. Since we no longer have a simple dominant poles situation, a time response simulation is needed to assess the design. Before this is undertaken, the effect of a higher gain in the roll-rate loop will be considered.

If the roll-rate loop is closed, with $k_p = 0.4$, the roll subsidence pole moves out to $s = -3.08$, and the zero in the yaw-rate loop transfer function (1) moves from $s = -0.76$ to $s = -3.40$. This causes different behavior in the root-locus plot for the yaw-rate loop, as shown in Figure 4.4-8. The washout pole now moves to the left instead of the right. A comparison of Figures 4.4-7 and 4.4-8 shows that the price paid for this potential improvement in roll response is that the maximum dutch roll frequency is reduced. If the yaw-rate loop is closed with $k_r = 1.3$, to obtain the highest possible damped frequency for the dutch roll poles, the closed-loop transfer functions are

$$\frac{p}{r_1} = \frac{119.4(s+19.27)(s+1.74)(s-0.0507)(s+0.334\pm j0.787)}{(s+19.25)(s+17.4)(s+0.00767)(s+2.82)(s+1.57)(s+0.987\pm j0.984)} \quad (4)$$

$$\frac{r}{r_2} = \frac{12.40(s+1.00)(s+17.1)(s+3.40)(s+0.486\pm j0.459)}{(s+19.25)(s+17.4)(s+0.00767)(s+2.82)(s+1.57)(s+0.987\pm j0.984)} \quad (5)$$

The dutch roll frequency has decreased to $\omega_n = 1.39$ rad/s, and the damping has increased to $\zeta = 0.71$; these values still represent good flying qualities (see Table 4.3-6). An improvement in the roll response should have been obtained since the slow washout pole is nearly canceled by the zero at $s = -1.74$, and the roll

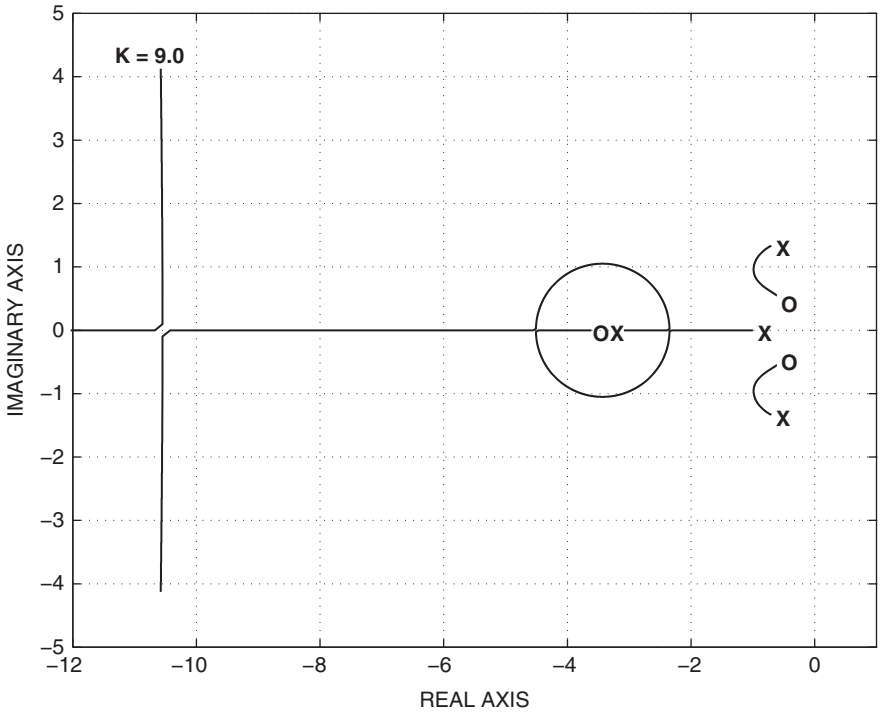


**Figure 4.4-8** Alternate yaw-rate root locus.

subsidence pole (at $s = -2.82$) may now dominate the roll response. Note the way in which one actuator pole almost cancels out of each transfer function. Also, in the yaw-rate response, note the zero at $s = -1$ that originally canceled the washout pole. The transfer functions still show significant roll-yaw coupling.

The roll response of this design can only be assessed with a simulation, and because of the presence of the slow spiral pole in the transfer functions, a doublet pulse should be used as the input. The time responses were obtained by closing the yaw-rate and roll-rate loops with the feedback gains above ($k_p = 0.4, k_r = 1.3$) and using the following commands:

```
acl2= a - b*[.4 0; 0 1.3]*c;                % Close roll & yaw
t= [0:.02:10];                              % 501 points for plot
u= [-1.8*ones(1,51),1.8*ones(1,50),zeros(1,400)]'; % Doublet
[y,x]= lsim(acl2,b(:,1),c(1,:),0,u,t);      % Linear simulation
plot(t,y,t,u)
grid on
```

Figure 4.4-9 compares the roll-rate response of the open-loop dynamics (augmented with the actuators) with the closed-loop response. The doublet input is negative for 1 s, positive for 1 s, then zero, with unit amplitude in the open-loop case. In the

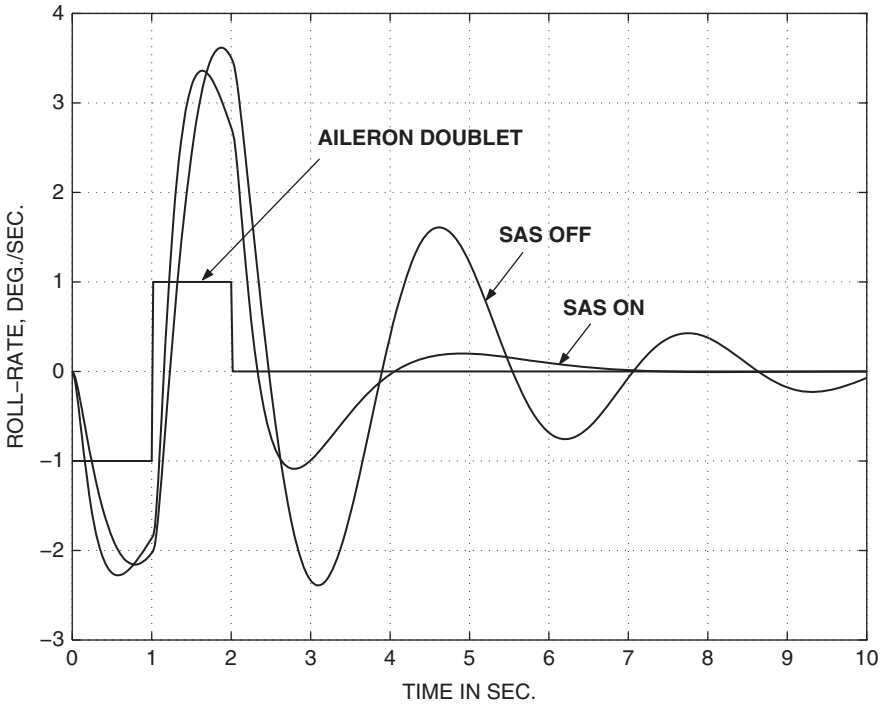


**Figure 4.4-9** Roll-rate response to an aileron doublet.

closed-loop case the overall gain is different, and the doublet was adjusted to 1.8° so that the responses were of similar amplitude. The figure exhibits the major improvement in the dutch roll damping and the small but significant improvement in the roll-rate speed of response. ■

This example indicates the difficulties of multivariable design when significant cross-coupling is present in the dynamics. It also shows the difficulty of obtaining a good roll response at low dynamic pressure and high alpha. The design could be pursued further by investigating the effect of changing the washout time constant and using compensation networks, such as a phase lead, in the yaw-rate feedback loop. As pointed out earlier, increasing the bandwidth of the control loops may simply lead to saturation of the control surface actuators, and the limitations of the basic aircraft must be considered first.

## 4.5 CONTROL AUGMENTATION SYSTEMS

When an aircraft is under manual control (as opposed to autopilot control), the stability augmentation systems of the preceding section are, in most cases, the only automatic flight control systems needed. But in the case of high-performance military